american physiological society

JNP JOURNAL OF NEUROPHYSIOLOGY

J Neurophysiol 135: 815–823, 2026.
First published March 4, 2026; doi:10.1152/jn.00519.2025

SHORT REPORT

Neural Circuits

Serotonergic modulation of cortical gamma synchronization: right-lateralized psilocin effects on 40 Hz auditory steady-state responses in rats

Inga Griškova-Bulanova,[1,2,3] Čestmír Vejmola,[1,4] and Tomáš Páleníček[1,4]

[1]*Psychedelic Research Centre, National Institute of Mental Health, Klecany, Czech Republic;* [2]*Institute of Biosciences, Vilnius University, Vilnius, Lithuania;* [3]*Translational Health Research Institute, Vilnius University, Vilnius, Lithuania; and* [4]*Third Faculty of Medicine, Charles University, Praha, Czech Republic*

Abstract

Auditory steady-state responses (ASSRs), particularly at 40 Hz, are promising biomarkers for psychiatric disorders involving dysregulated neural synchronization. Although most ASSR studies have focused on the glutamatergic system, the serotonergic system, specifically 5-HT2A receptor signaling, has received limited attention. Psilocin, the active metabolite of psilocybin and a known 5-HT2A receptor agonist, alters cortical oscillatory activity, but its effects on ASSR dynamics remain unclear. In this study, we examined psilocin's effects on ASSRs in eight adult male Wistar rats implanted with 21 cortical electrodes. The rats were exposed to 40 Hz and 80 Hz click-train stimulation before and 30 min after subcutaneous psilocin administration (4 mg/kg). EEG signals were analyzed using time-frequency decomposition to extract phase-locking index (PLI) and event-related spectral perturbation (ERSP) values from frontal and temporal regions of both hemispheres. Psilocin selectively decreased PLI at 40 Hz stimulation in the right temporal cortex, with no significant changes in the frontal or left temporal regions, nor in response to 80 Hz stimulation. ERSP analysis revealed a global reduction in spectral power after psilocin administration in response to 80 Hz stimuli, but no consistent effects at 40 Hz. These results indicate that psilocin induces region- and frequency-specific alterations in auditory neural synchronization, characterized by right-lateralized disruption of 40 Hz phase-locking. This highlights the sensitivity of low-gamma oscillations to serotonergic modulation and supports the use of ASSR paradigms in translational models of altered perceptual and cognitive states.

NEW & NOTEWORTHY This is the first preclinical study to demonstrate that psilocin selectively disrupts auditory steady-state responses (ASSRs) in rats in a frequency- and region-specific manner. The findings indicate a right-lateralized reduction in phase-locking at 40 Hz, along with a global suppression of spectral power at 80 Hz. These results provide new insights into the serotonergic modulation of neural synchrony and support the use of ASSRs as a translational biomarker for altered perceptual states.

auditory steady-state response; gamma oscillations; neural synchrony; psilocin; rats

INTRODUCTION

In recent years, there has been a growing interest in identifying biomarkers for psychiatric disorders that can help predict and monitor brain states. One promising candidate is the auditory steady-state response (ASSR), which demonstrates good translational validity between animal models and humans (1).

ASSR resembles a periodic response to auditory periodic stimulation and is used to test the capabilities of the brain to generate activity in a certain frequency range (2). The 40 Hz ASSR is particularly relevant, as impairments in this frequency have been consistently documented in patients with schizophrenia (3) and bipolar disorder (4). In contrast, the evidence surrounding ASSR in individuals with autism spectrum disorder remains less definitive, with results exhibiting considerable variability (5, 6). Moreover, investigations have revealed that patients with schizophrenia (7–9) and bipolar disorder (10) also demonstrate altered responses at elevated frequency ranges exceeding 80 Hz. This altered neural activity is believed to originate from distinct cortical networks, where local superficial

Correspondence: I. GriŠkova-Bulanova (inga.griskova-bulanova@gf.vu.lt).
Submitted 17 October 2025 / Revised 15 December 2025 / Accepted 24 February 2026

networks are implicated in the generation of low-gamma range ASSRs (30–50 Hz) (11), while subcortical structures, including the brainstem and thalamus, contribute to the modulation of 80 Hz ASSRs (12–14). Consequently, the exploration of both lower and higher frequency ASSRs may provide critical insights into the complex electrophysiological alterations observed in various neuropsychiatric conditions.

Due to the simplicity of the ASSR paradigm for human subjects and the ease of its translational aspects, this response is frequently studied in animal models as well (15). Nevertheless, the neurochemical mechanisms of the gamma-range ASSRs are still not fully understood. Previous studies on the neurochemical background of ASSR have mostly focused on the NMDA system that is implicated in psychosis (16, 17). 40 Hz ASSRs were shown as a possible biomarker of cortical NMDA function, supporting the glutamatergic hypothesis of schizophrenia (17, 18). NMDA antagonists (ketamine, MK-801, and phencyclidine) were shown both to reduce low gamma-range ASSR (17, 19–21) and to increase it (15, 22, 23) in a dose-dependent manner. However, studies utilizing high-frequency range ASSR are scarce and inconclusive. At the same time, the recent view on the neurochemical alterations in psychosis suggests the important involvement of dopamine (24) and serotonin (25) systems, whose contribution to ASSRs is not clear. This knowledge is important for the correct interpretation of the findings and estimation of a better relationship to disorder-related alterations.

In this study, we address the local (electrode-level) effects of 5-HT2A receptor agonist psilocin on the low (40 Hz) and high (80 Hz) frequency ASSRs. We hypothesize that a disruptive effect on ASSR will be evident based on previous reports in animal models on the broadband gamma activity (26), similar to the effect on 40 Hz ASSR reported in humans (27). We are specifically interested in evaluating response in frontal and temporal regions, as several reports demonstrated differential behavior of ASSR in these two regions in animal models (15, 16, 28). We also aimed to assess potential laterality-related effects of the response, as in humans, right-sided dominance of ASSRs was demonstrated (29, 30), and rats have a well-pronounced functional laterality of the auditory cortex (31, 32). Thus, we hypothesize that ASSRs will be affected by psilocin administration and the neural response itself, with the psilocin effects being more pronounced in the temporal regions, potentially exhibiting lateralization.

MATERIALS AND METHODS

Animals

All procedures were conducted in accordance with the Guiding Principles for the Care and Use of Vertebrate Animals in Research and Training, and approved by the Czech National Committee for the Care and Use of Laboratory Animals. Experiments were performed on 8 adult male Wistar rats (RRID: RGD_13508588), weighing ∼300 g at the start of the experiment (SPF animals; Velaz, Czech Republic). Each animal was used in one experimental session only. Animals were housed individually postsurgery in standard cages, maintained on a 12-h light/dark cycle with ad libitum access to food and water. Daily handling was carried out for habituation to minimize stress.

Drugs

Psilocin was synthesized and supplied by the Forensic Laboratory of Biologically Active Compounds, University of Chemistry and Technology, Prague, Czech Republic. The compound was dissolved in 0.9% NaCl (B. Braun, Germany) with the addition of glacial acetic acid (Penta Chemicals, Czech Republic; 5 µL/20 mL) to enhance solubility. The solution was prepared fresh each experimental day. A subcutaneous injection of 4 mg/kg psilocin was administered at a volume of 2 mL/kg.

Surgery

Seven days before EEG recording, animals were anesthetized with isoflurane (2.5%, Isoflurane Vetpharma) and stereotactically implanted with 21 epidural gold-plated electrodes (Mill-Max Mfg. Corp., NY) positioned over the cortical surface using coordinates from the Paxinos and Watson rat brain atlas (33). Electrodes targeted homologous regions of the frontal, temporal, and parietal cortex in both hemispheres. The reference electrode was placed over the olfactory bulb, and the ground electrode was implanted subcutaneously in the occipital region. All electrodes were fixed to the skull with dental cement (Dentalon Plus, Heraeus Kulzer). Postoperative analgesia was provided via ketoprofen (5 mg/kg, sc, Bioveta, Czech Republic), which was administered once per day for four days following surgery. Rats were housed individually postsurgery to prevent damage to the implant, and connectors were attached under brief anesthesia the day before recording.

Auditory Stimulation and EEG Recording

Rats were habituated for three consecutive days to the recording conditions and auditory stimulation. Habituation consisted of exposure to a full 20-min ASSR stimulation sequence played in the same room, under identical acoustic and environmental conditions as used during the actual EEG recordings. Although the animals were connected to an EEG amplifier during this sham stimulation, no EEG data were recorded. The purpose of this procedure was to familiarize the animals with the auditory stimuli and experimental environment, thereby reducing novelty- and stress-related confounds during the recording sessions. Recordings were performed in the home cage while animals were freely moving. Auditory stimuli were delivered via stereo speakers positioned on both sides of the cage. The ASSR protocol consisted of 1-s trains of auditory clicks (90 dB SPL) delivered at 40 and 80 Hz with randomized interstimulus intervals (2–4 s). Each frequency was presented in pseudo-randomized blocks in two 20-min sessions separated by a 10-min pause. In total, 120 trains per frequency were delivered per session. The schematic representation of the experiment flow is presented in Fig. 1. After the baseline session, psilocin was injected, and the same protocol was repeated 30 min later. EEG recordings were performed using a tethered recording system. Animals were connected via a lightweight, flexible cable to a BioSDA09 standard 32-channel digital EEG amplifier (M&I Ltd., Prague, Czech Republic), allowing free movement within the home cage during recording. Signals were acquired at a sampling rate of 5000 Hz and stored for offline analysis. All EEG recordings were

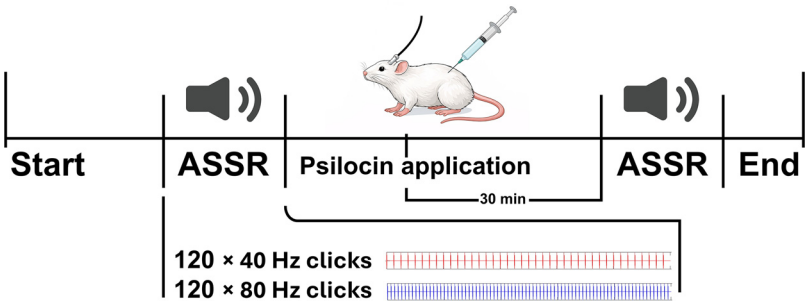

Figure 1. Experimental timeline of the auditory steady-state response (ASSR) protocol. Rats underwent baseline ASSR recording (120 click trains at 40 Hz), followed by psilocin administration (4 mg/kg, sc) and a second ASSR session after a 30-min interval.

conducted between 7:00 PM and 11:00 PM, corresponding to the active (dark) phase of the rats' circadian cycle.

EEG Preprocessing

EEG data were processed using BrainVision Analyzer 2 (Brain Products GmbH, Germany). Raw data were filtered (1–200 Hz, 8th-order IIR bandpass filter) and a 50 Hz notch filter applied. Artifact rejection was performed via visual inspection by a trained researcher. Channels were rereferenced to the average of all non-noisy electrodes. Stimulus-locked epochs from −700 to +1500 ms were extracted, and trials were concatenated for each stimulation frequency to create continuous signals. These were then exported in EEGLAB format for further analysis.

Time-Frequency Analysis

Analysis was conducted in MATLAB (R2021a, MathWorks Inc.) using the ERPWAVELAB toolbox. Data from four electrodes (Fp1, Fp2, T3, T4) were analyzed. A complex Morlet wavelet transform (7-cycle) was applied to obtain power and phase measures from 1 to 100 Hz in 1-Hz steps. We focused on two outcome measures: *1*) Phase-locking index (PLI), indexing inter-trial phase consistency, and *2*) Event-related spectral perturbation (ERSP), reflecting amplitude modulations induced by stimulation. To isolate late-latency gamma activity (34), mean values were extracted from 200 to 900 ms poststimulus. For 40 Hz stimuli, 35–45 Hz frequency bands were analyzed; for 80 Hz stimuli, 75–85 Hz bands. Both PLI and ERSP were baseline-corrected relative to the −500 to −100 ms prestimulus period.

Statistical Analysis

Statistical analyses were restricted a priori to frontal (Fp1, Fp2) and temporal (T3, T4) electrodes based on predefined hypotheses supported by the observed topographical patterns (Fig. 2). To assess the effect of psilocin on ASSR, repeated-measures ANOVA (RM-ANOVA) was used with three within-subject factors: Psilocin (Pre, Post), Region (Frontal, Temporal), and Hemisphere (Left, Right). A priori planned contrasts were defined as follows: *1*) Psilocin effect: Pre versus Post difference across all conditions; *2*) Psilocin × Region: Differential drug effect in frontal versus temporal regions; *3*) Psilocin × Region × Hemisphere: Lateralized regional effects of drug. Each contrast was tested using paired-sample *t*-tests. Effect sizes were reported using Cohen's *d* and 95% confidence intervals. For significant interactions involving Hemisphere, separate comparisons were conducted per region. Pearson correlation was used to assess relationships between baseline values and drug-induced changes. Analyses were conducted in MATLAB and JASP (version 0.19.1; https://jasp-stats.org).

RESULTS

This study examined the effects of psilocin administration on neural synchronization, as measured by the phase-locking index (PLI) and event-related spectral perturbation (ERSP) in response to 40 Hz and 80 Hz auditory steady-state stimulation. Descriptive statistics are summarized in Table 1, and results of repeated-measures ANOVA are summarized in Table 2.

For 40 Hz PLI, a repeated-measures ANOVA revealed a significant main effect of region [$F(1,7) = 18.675$, $P = 0.003$, $\eta_p^2 = 0.727$], indicating higher synchronization in temporal than frontal areas. The interaction between psilocin and region was not significant [$F(1,7) = 0.740$, $P = 0.418$, $\eta_p^2 = 0.096$]. No significant main effects were observed for psilocin [$F(1,7) = 0.560$, $P = 0.479$, $\eta_p^2 = 0.074$] or hemisphere [$F(1,7) = 0.096$, $P = 0.766$, $\eta_p^2 = 0.013$], suggesting that neither overall psilocin administration nor hemispheric laterality had a global effect on PLI. However, we found a significant psilocin × hemisphere interaction [$F(1,7) = 6.601$, $P = 0.037$, $\eta_p^2 = 0.485$], and a significant psilocin × region × hemisphere interaction [$F(1,7) = 7.576$, $P = 0.028$, $\eta_p^2 = 0.520$], indicating that psilocin's effects were spatially specific and varied across hemispheres and regions. Descriptive values (Table 1) indicate that these interactions were driven by a reduction in 40 Hz PLI in the right temporal hemisphere following psilocin administration, whereas no corresponding change was observed in the left hemisphere.

Planned contrasts supported these observations. The main effect of psilocin on PLI was not significant ($t_7 = -0.748$, $P = 0.479$, $d = -0.230$, 95% CI [−0.722, 0.375]), nor was the psilocin × region interaction ($t_7 = 0.860$, $P = 0.418$, $d = 0.441$). However, the psilocin × region × hemisphere interaction contrast was significant ($t_7 = -2.753$, $P = 0.028$, $d = -1.584$, 95% CI [−2.227, −0.169]), confirming that psilocin's influence on PLI was spatially and laterally specific.

To further localize these effects, we performed separate ANOVAs for frontal and temporal electrodes. In the temporal region, we observed a significant psilocin × hemisphere interaction [$F(1,7) = 7.446$, $P = 0.029$, $\eta_p^2 = 0.515$], indicating that psilocin effects differed across hemispheres. No significant effects were observed in the frontal region. Follow-up paired-sample t-tests showed no significant change in left temporal PLI ($t_7 = -0.556$, $P = 0.596$, $d = -0.196$, 95% CI [−0.890, 0.511]), but a significant decrease in right

temporal PLI following psilocin ($t_7 = 2.603$, $P = 0.035$, $d = 0.920$, 95% CI [0.060, 1.738]), indicating lateralized reduction in synchronization.

For 80 Hz PLI, the repeated-measures ANOVA revealed a significant main effect of region [$F(1,7) = 13.089$, $P = 0.009$, $\eta_p^2 = 0.652$], with higher values in temporal than frontal areas. However, the main effect of psilocin [$F(1,7) = 0.000364$, $P = 0.985$, $\eta_p^2 = 5.20\text{e-}05$] was not significant, nor were the psilocin × region [$F(1,7) = 0.320$, $P = 0.589$, $\eta_p^2 = 0.045$] or psilocin × hemisphere [$F(1,7) = 0.105$, $P = 0.755$, $\eta_p^2 = 0.015$] interactions. The three-way psilocin × region × hemisphere interaction was also not significant [$F(1,7) =$

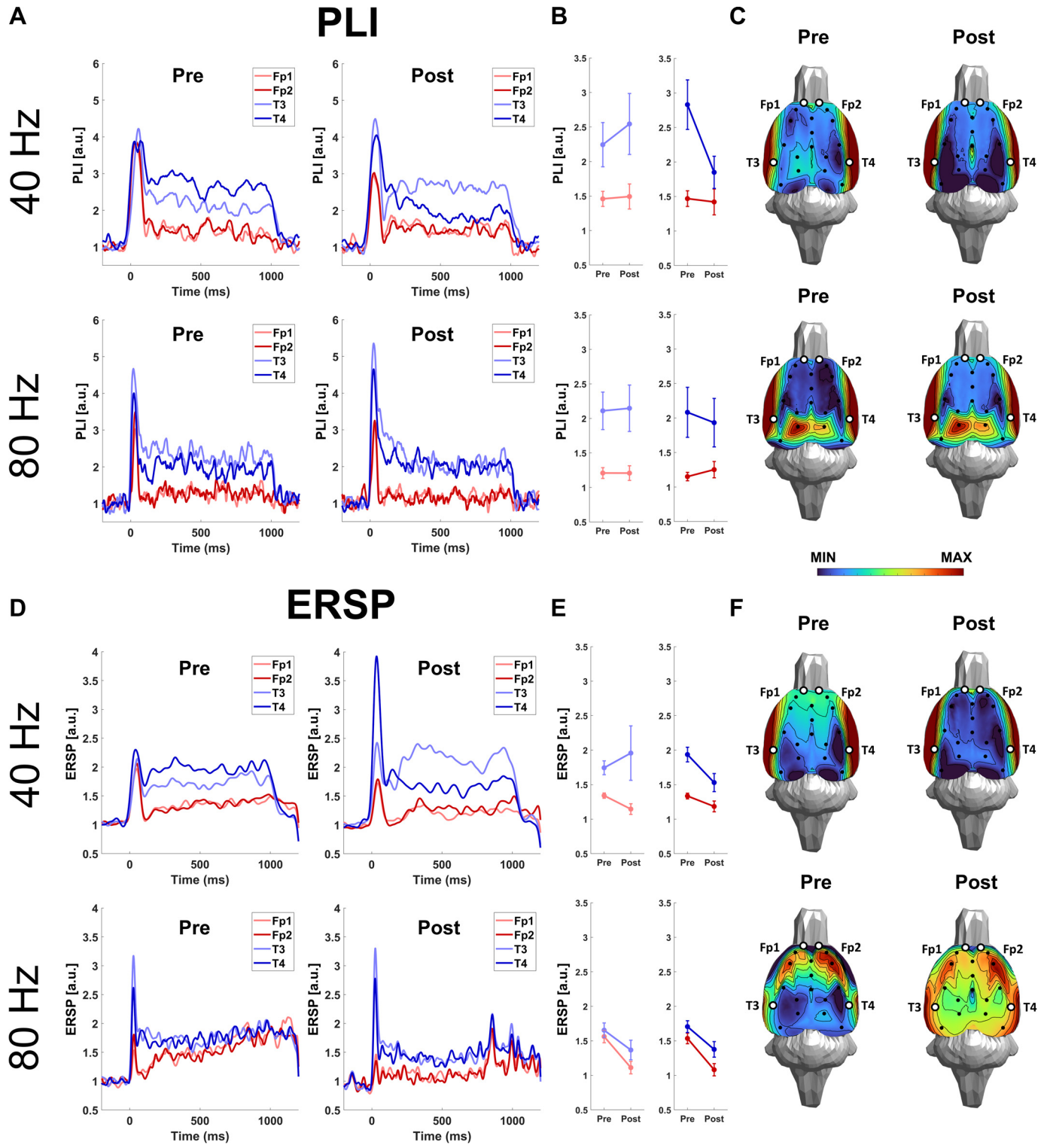

Table 1. *Descriptive statistics of PLI and ERSP values*

				PLI		ERSP	
	Drug	Region	Hemisphere	Means	SE	Means	SE
40 Hz ASSR	Pre	Frontal	Left	1.459	0.109	1.341	0.038
			Right	1.469	0.113	1.335	0.041
		Temporal	Left	2.244	0.32	1.744	0.1
			Right	2.83	0.358	1.936	0.106
	Post	Frontal	Left	1.493	0.182	1.146	0.077
			Right	1.421	0.187	1.184	0.078
		Temporal	Left	2.544	0.441	1.957	0.394
			Right	1.85	0.233	1.53	0.131
80 Hz ASSR	Pre	Frontal	Left	1.209	0.078	1.562	0.09
			Right	1.151	0.061	1.535	0.077
		Temporal	Left	2.11	0.271	1.654	0.105
			Right	2.082	0.362	1.706	0.085
	Post	Frontal	Left	1.208	0.106	1.112	0.09
			Right	1.252	0.118	1.081	0.089
		Temporal	Left	2.147	0.336	1.367	0.142
			Right	1.932	0.351	1.376	0.113

Means and standard error (SE) values for PLI and ERSP in response to 40 Hz and 80 Hz auditory steady-state stimulation, reported separately for each condition (Pre/Post), brain region (Frontal/Temporal), and hemisphere (Left/Right). ASSR, auditory steady-state response; ERSP, event-related spectral perturbation; PLI, phase-locking index.

2.323, $P = 0.171$, $\eta_p^2 = 0.249$]. Planned contrasts confirmed these results, with no significant change in PLI following psilocin administration ($t_7 = -0.019$, $P = 0.985$, $d = -0.007$, 95% CI [−0.507, 0.502]).

For 40 Hz ERSP, a repeated-measures ANOVA showed a significant main effect of region [$F(1,7) = 14.179$, $P = 0.007$, $\eta_p^2 = 0.669$], indicating higher evoked spectral power in temporal areas. The psilocin × region × hemisphere interaction was also significant [$F(1,7) = 6.273$, $P = 0.041$, $\eta_p^2 = 0.473$]. However, the main effect of psilocin [$F(1,7) = 1.079$, $P = 0.333$, $\eta_p^2 = 0.134$] and the psilocin × region interaction [$F(1,7) = 0.197$, $P = 0.670$, $\eta_p^2 = 0.027$] were not significant. The planned contrast for the three-way interaction was significant ($t_7 = -2.505$, $P = 0.041$, $d = -1.451$, 95% CI [−2.177, −0.057]), suggesting region- and hemisphere-dependent psilocin effects. When analyzing regions separately, the frontal region showed a trend-level main effect of psilocin [$F(1,7) = 4.767$, $P = 0.065$], and the temporal region showed a trend-level psilocin × hemisphere interaction [$F(1,7) = 4.264$, $P = 0.078$], suggesting potential spatial specificity in psilocin's influence on spectral power.

Finally, for 80 Hz ERSP, we found a significant main effect of drug [$F(1,7) = 9.014$, $P = 0.020$, $\eta_p^2 = 0.563$], indicating a global decrease in spectral power following psilocin administration. Region [$F(1,7) = 4.728$, $P = 0.066$, $\eta_p^2 = 0.403$] and hemisphere [$F(1,7) = 0.00021$, $P = 0.989$, $\eta_p^2 = 3.00\text{e-}05$] effects were not significant, and there were no significant interactions involving these factors. The planned contrast confirmed a significant decrease in ERSP postpsilocin ($t_7 = -3.002$, $P = 0.020$, $d = -1.261$, 95% CI [−2.180, −0.269]), supporting a general suppressive effect of psilocin at 80 Hz that was not spatially specific.

DISCUSSION

We aimed to evaluate the effect of a single acute dose of psilocin on the ability to generate evoked responses at 40 Hz and 80 Hz in Wistar rats. The utilization of the ASSR approach allowed us to assess the generation capacity of both low and high gamma activity, similar to studies performed in humans, where both low and high gamma were demonstrated to be impaired in conditions associated with psychosis (6–9) and associated with the severity of hallucination in patients with schizophrenia (35, 36). In our study, psilocin induced a selective, frequency- and region-specific modulation of auditory steady-state responses in rats. The psilocin reduced 40 Hz phase-locking specifically in the right temporal cortex, indicating lateralized disruption of low-gamma neural synchrony, whereas 80 Hz phase-locking remained preserved. In contrast, 80 Hz spectral power was reduced in both frontal and temporal regions, revealing dissociation between phase precision and amplitude.

Previously, psilocin has been shown to induce a global reduction of broadband EEG activity, including low-gamma power, in rats at the same dosage as used in the present

Figure 2. Group-level results of auditory steady-state responses (ASSRs) at 40 Hz and 80 Hz. *A*: grand-average time courses of PLI in response to 40 Hz (*top*) and 80 Hz (*bottom*) stimulation, shown separately for frontal (Fp1, Fp2) and temporal (T3, T4) electrodes before (Pre) and after (Post) psilocin administration. Traces represent averages across all animals and trials; values are expressed as ratios relative to the prestimulus baseline. *B*: mean PLI values (means ± SE) averaged across the late response window (200–900 ms) and frequency bands of interest (35–45 Hz for 40 Hz stimulation; 75–85 Hz for 80 Hz stimulation). Data are shown separately for frontal and temporal electrodes and for left and right hemispheres. Points represent group means from all animals ($n = 8$). *C*: topographical distribution of PLI across the full electrode array for 40 Hz (*top*) and 80 Hz (*bottom*) stimulation before and after psilocin administration. The four electrodes included in the statistical analysis (Fp1, Fp2, T3, T4) are highlighted. Color scales represent relative PLI values and were independently scaled to the minimum and maximum values within each condition to emphasize spatial patterns. *D*: grand-average time courses of ERSP in response to 40 Hz (*top*) and 80 Hz (*bottom*) stimulation for frontal and temporal electrodes before and after psilocin administration. ERSP values are expressed as ratios relative to baseline. *E*: mean ERSP values (means ± SE) averaged across the same time–frequency windows as in *B*, shown separately for region and hemisphere ($n = 8$). *F*: topographical maps of ERSP for 40 Hz (*top*) and 80 Hz (*bottom*) stimulation before and after psilocin administration. As in *C*, the four analyzed electrodes are highlighted, and colormaps were scaled to the minimum and maximum values within each condition. ERSP, event-related spectral perturbation; PLI, phase-locking index.

Table 2. *Results of repeated-measures ANOVA for PLI and ERSP*

	Effect	PLI			ERSP		
		F	*P*	η_p^2	*F*	*P*	η_p^2
40 Hz ASSR	Drug	0.56	0.479	0.074	1.079	0.333	0.134
	Region	18.675	0.003*	0.727	14.179	0.007*	0.669
	Hemisphere	0.096	0.766	0.013	0.352	0.572	0.048
	Drug × Region	0.74	0.418	0.096	0.197	0.67	0.027
	Drug × Hemisphere	6.601	0.037*	0.485	2.923	0.131	0.295
	Region × Hemisphere	0.008	0.932	0.001	0.438	0.529	0.059
	Drug × Region × Hemisphere	7.576	0.028*	0.52	6.273	0.041*	0.473
80 Hz ASSR	Drug	0.000364	0.985	5.20e-05	9.014	0.02*	0.563
	Region	13.089	0.009*	0.652	4.728	0.066	0.403
	Hemisphere	0.122	0.737	0.017	0.00021	0.989	3.00e-05
	Drug × Region	0.32	0.589	0.044	1.291	0.293	0.156
	Drug × Hemisphere	0.105	0.755	0.015	1.613	0.245	0.187
	Region × Hemisphere	0.106	0.754	0.015	0.528	0.491	0.07
	Drug × Region × Hemisphere	2.323	0.171	0.249	0.259	0.626	0.036

F values, *P* values, and partial eta-squared (η_p^2) are reported for main effects and interactions of Drug, Region, and Hemisphere in response to 40 Hz and 80 Hz auditory steady-state stimulation. Asterisks (*) indicate statistically significant effects ($P < 0.05$). Significant Drug × Hemisphere and Drug × Region × Hemisphere interactions at 40 Hz are driven by a postdrug reduction in phase-locking in the right temporal hemisphere (Table 1 and Fig. 2). ASSR, auditory steady-state response; ERSP, event-related spectral perturbation; PLI, phase-locking index.

study (26). Our results extend these findings by demonstrating frequency-, region-, and hemisphere-specific modulation of auditory steady-state responses, supporting the involvement of serotonergic mechanisms and 5-HT2A receptor–mediated modulation of ASSR circuits, in line with our recent human study (27). Importantly, no global effect of psilocin on phase-locking indices was observed. Instead, psilocin selectively affected low-gamma synchronization, with a significant lateralized reduction of 40 Hz PLI in the right temporal region but not in frontal sites, indicating regionally specific disruption of temporal coordination. Although psilocin is primarily considered a 5-HT2A receptor agonist (37), receptor specificity was not directly tested in the present study, as no selective antagonists were used. Therefore, the receptor-level interpretation remains inferential and warrants future validation.

Notably, ERSP and PLI capture complementary aspects of ASSRs: ERSP reflects overall oscillatory power and is more sensitive to noise and amplitude fluctuations, whereas PLI indexes the temporal precision of phase-locked neural responses and is more stable over time (38, 39). Consistent with this distinction, the lack of psilocin effects on PLIs at 80 Hz suggests that higher-frequency gamma synchronization is relatively resistant to serotonergic desynchronization. Nevertheless, a reduction in 80 Hz ERSP was observed, in agreement with previously reported broadband EEG attenuation following psilocin administration (26). Within the ASSR framework, however, these effects were not global but instead frequency- and region-specific.

Low-gamma ASSRs around 40 Hz are generated predominantly within superficial cortical networks, whereas high-gamma responses near 80 Hz rely more strongly on subcortical and thalamocortical circuits (12–14). Although 5-HT2A receptors are expressed in both cortex and thalamus (40, 41), our results indicate that psilocin selectively disrupts cortically generated 40 Hz synchronization while sparing the temporal coordination of subcortically supported 80 Hz responses. Importantly, despite reduced 80 Hz ASSR power, phase-based synchronization metrics remained preserved, indicating attenuation of oscillatory strength without disruption of temporal precision. The lack of effect on 80 Hz PLI, despite the ERSP reduction, raises questions about whether higher gamma frequencies are less susceptible to serotonergic modulation. The effects observed at 40 Hz but not 80 Hz may relate to differential serotonergic modulation of inhibitory interneurons, where psilocin's influence on 5-HT2A receptor-mediated disinhibition may preferentially impact lower gamma frequencies. Alternatively, the preserved 80 Hz phase-locking may reflect greater robustness of high-gamma synchronization rather than reduced serotonergic sensitivity per se, a distinction that cannot be resolved within the present design.

Overall, only a few studies to date have utilized the ASSR approach to study serotonergic modulation, with almost all being conducted in humans, making it difficult to discuss the observed outcomes. Apart from our previous study in humans, which demonstrated reduced PLIs after a single dose of psilocybin, whose active metabolite psilocin acts primarily as a 5-HT2A receptor agonist with additional affinity for 5-HT1A receptors (27), Nissen et al. reported a reduction in gamma-band evoked power after serotonin reuptake inhibitors, including vortioxetine and escitalopram (42). In a Fragile X Syndrome mouse model, the selective 5-HT1A agonist NLX-101 was recently reported to restore 40 Hz PLI (43). No effect of the selective 5-HT3R antagonist CVN058 was observed on 40 Hz ASSR in humans (44). This indicates the need for further research.

We observed a right-lateralized decrease in 40 Hz PLI, whereas the response in the left temporal region remained statistically unchanged. This pattern is consistent with prior studies demonstrating hemispheric asymmetries in auditory neural dynamics in rats. Functional lateralization of the rodent auditory system has been reported previously, with the left auditory cortex preferentially involved in detecting fine temporal elements, such as gap durations (45) or specific vocalization features (46), while the right auditory cortex integrates broader spectro-temporal information (45, 46). Notably, an asymmetric distribution of 40 Hz ASSRs is also

well-documented in humans, with responses typically more pronounced over the right hemisphere (29, 30, 47).

Psilocin, the active metabolite of psilocybin, is known to induce psychotic-like perceptual alterations in humans (48). In our previous human study, greater hallucinogenic intensity was associated with reduced 40 Hz ASSR PLI following psilocybin administration (27). At the same psilocin dosage used here (4 mg/kg), hallucination-like behavior has also been reported in rats (49). Moreover, human studies have demonstrated associations between altered 40 Hz phase-locking and auditory hallucination severity, with aberrant and often lateralized ASSR responses observed in patients with schizophrenia (36, 50, 51). Given that gamma oscillations, and gamma-range ASSRs in particular, are closely linked to cognitive processing (52), perceptual integration (53), and altered states of consciousness (54, 55), the selective modulation of 40 Hz synchronization observed here may reflect functionally meaningful changes in neural dynamics and stand as a translationally relevant neural signature associated with psychotic-like perceptual and cognitive alterations across species. However, as we did not assess behavioral correlates of psychosis-like states after psilocin, these links should be considered hypothesis-generating rather than conclusive.

A limitation of the present study is that the primary effects emerged through region- and hemisphere-specific interaction terms rather than global main effects, which may increase statistical uncertainty in a small-sample preclinical design relying on a single electrophysiological modality. These findings should therefore be interpreted with appropriate caution. Nevertheless, the observed effects were associated with relatively large effect sizes. Moreover, the behavioral and neurophysiological effects of this psilocin dose are well characterized in rodent models, and the present work was designed to provide a translational analogue of human ASSR measurements rather than to comprehensively characterize behavioral or multimodal outcomes.

Conclusions

This study demonstrates that psilocin selectively modulates auditory steady-state responses in rats in a frequency- and region-specific manner. Although no global changes were observed in phase-locking at 40 Hz, a significant right-lateralized reduction in temporal synchronization was detected, indicating localized sensitivity of low gamma oscillations to serotonergic modulation. In contrast, 80 Hz phase-locking remained unaffected, though spectral power in this range decreased globally. These results suggest that psilocin affects the precision and amplitude of auditory-driven neural oscillations through distinct mechanisms, likely reflecting differential involvement of cortical and subcortical generators and their receptor-level modulation. The lateralized disruption at 40 Hz may be particularly relevant to models of altered perception and consciousness, supporting the utility of rodent ASSRs as translational biomarkers for investigating serotonergic contributions to psychiatric symptomatology.

DATA AVAILABILITY

The datasets generated and analyzed during the current study are available from the corresponding author upon reasonable request. Data are not publicly available due to ethical restrictions regarding animal data sharing.

ACKNOWLEDGMENTS

The authors thank Stanislav Jiříček for his support with data analysis, particularly for sharing the script used to generate topographical maps. The authors also acknowledge Jacques Leca for his valuable assistance during data collection and Evaldas Pipinis for his help with data analysis, specifically in implementing the time-frequency analysis.

GRANTS

This work was supported by the ERDF-Project Brain Dynamics (No. CZ.02.01.01/00/22_008/0004643), and by the Czech Science Foundation (Project No. 23–07578 K).

DISCLAIMERS

All experimental procedures were conducted in accordance with the ethical standards for the care and use of laboratory animals. The study protocol was reviewed and approved by the National Committee for the Care and Use of Laboratory Animals, Czech Republic, under EU Directive 86/609/EEC. Ethical approval was granted by the Institutional Animal Care and Use Committee of the National Institute of Mental Health, Klecany, Czech Republic (protocol number available upon request).

DISCLOSURES

Dr. Tomáš Páleníček declares shares in "Psychedelická klinika s.r.o.", is the founder of "PSYRES – Psychedelic Research Foundation," holds shares in "Společnost pro podporu neurovědního výzkumu s.r.o.," and is involved in clinical trials with psilocybin conducted by Compass Pathways. He is also a collaborator in MAPS clinical trials with MDMA and reports consulting fees from GH Research and CB21-Pharma outside the submitted work. None of the other authors has any conflicts of interest, financial or otherwise, to disclose.

AUTHOR CONTRIBUTIONS

I.G.-B. and T.P. conceived and designed research; Č.V. performed experiments; I.G.-B. and Č.V. analyzed data; I.G.-B. and Č.V. interpreted results of experiments; Č.V. prepared figures; I.G.-B. and Č.V. drafted manuscript; T.P. edited and revised manuscript; T.P. approved final version of manuscript.

REFERENCES

1. **Grent-'t-Jong T**, **Brickwedde M**, **Metzner C**, **Uhlhaas PJ.** 40-Hz auditory steady-state responses in schizophrenia: toward a mechanistic biomarker for circuit dysfunctions and early detection and diagnosis. *Biol Psychiatry* 94: 550–560, 2023. doi:10.1016/j.biopsych.2023.03.026.
2. **Griskova-Bulanova I**, **Sveistyte K**, **Bjekic J.** Neuromodulation of gamma-range auditory steady-state responses: a scoping review of brain stimulation studies. *Front Syst Neurosci* 14: 41, 2020. doi:10.3389/fnsys.2020.00041.
3. **Zouaoui I**, **Dumais A**, **Lavoie ME**, **Potvin S.** Auditory steady-state responses in schizophrenia: an updated meta-analysis. *Brain Sci* 13: 1722, 2023. doi:10.3390/brainsci13121722.
4. **Jefsen OH**, **Shtyrov Y**, **Larsen KM**, **Dietz MJ.** The 40-Hz auditory steady-state response in bipolar disorder: a meta-analysis. *Clin Neurophysiol* 141: 53–61, 2022. doi:10.1016/j.clinph.2022.06.014.
5. **Seymour RA**, **Rippon G**, **Gooding-Williams G**, **Sowman PF**, **Kessler K.** Reduced auditory steady state responses in autism spectrum disorder. *Mol Autism* 11: 56, 2020. doi:10.1186/s13229-020-00357-y.

6. **Ahlfors SP**, **Graham S**, **Bharadwaj H**, **Mamashli F**, **Khan S**, **Joseph RM**, **Losh A**, **Pawlyszyn S**, **McGuiggan NM**, **Vangel M**, **Hämäläinen MS**, **Kenet T.** No differences in auditory steady-state responses in children with autism spectrum disorder and typically developing children. *J Autism Dev Disord* 54: 1947–1960, 2024. doi:10.1007/s10803-023-05907-w.
7. **Alegre M**, **Molero P**, **Valencia M**, **Mayner G**, **Ortuño F**, **Artieda J.** A typical antipsychotics normalize low-gamma evoked oscillations in patients with schizophrenia. *Psychiatry Res* 247: 214–221, 2017. doi:10.1016/j.psychres.2016.11.030.
8. **Tsuchimoto R**, **Kanba S**, **Hirano S**, **Oribe N**, **Ueno T**, **Hirano Y**, **Nakamura I**, **Oda Y**, **Miura T**, **Onitsuka T.** Reduced high and low frequency gamma synchronization in patients with chronic schizophrenia. *Schizophr Res* 133: 99–105, 2011. doi:10.1016/j.schres.2011.07.020.
9. **Griskova-Bulanova I**, **Voicikas A**, **Dapsys K**, **Melynyte S**, **Andruskevicius S**, **Pipinis E.** Envelope following response to 440 hz carrier chirp-modulated tones show clinically relevant changes in schizophrenia. *Brain Sci* 11: 22, 2020. doi:10.3390/brainsci11010022.
10. **Isomura S**, **Onitsuka T**, **Tsuchimoto R**, **Nakamura I**, **Hirano S**, **Oda Y**, **Oribe N**, **Hirano Y**, **Ueno T**, **Kanba S.** Differentiation between major depressive disorder and bipolar disorder by auditory steady-state responses. *J Affect Disord* 190: 800–806, 2016. doi:10.1016/j.jad.2015.11.034.
11. **Plourde G.** Auditory evoked potentials. *Best Pract Res Clin Anaesthesiol* 20: 129–139, 2006. doi:10.1016/j.bpa.2005.07.012.
12. **Tichko P**, **Skoe E.** Frequency-dependent fine structure in the frequency-following response: The byproduct of multiple generators. *Hear Res* 348: 1–15, 2017. doi:10.1016/j.heares.2017.01.014.
13. **Farahani ED**, **Wouters J**, **van Wieringen A.** Contributions of non-primary cortical sources to auditory temporal processing. *Neuroimage* 191: 303–314, 2019. doi:10.1016/j.neuroimage.2019.02.037.
14. **Farahani ED**, **Wouters J**, **van Wieringen A.** Brain mapping of auditory steady-state responses: a broad view of cortical and subcortical sources. *Hum Brain Mapp* 42: 780–796, 2021. doi:10.1002/hbm.25262.
15. **Kozono N**, **Honda S**, **Tada M**, **Kirihara K**, **Zhao Z**, **Jinde S**, **Uka T**, **Yamada H**, **Matsumoto M**, **Kasai K**, **Mihara T.** Auditory steady state response; nature and utility as a translational science tool. *Sci Rep* 9: 8454, 2019. doi:10.1038/s41598-019-44936-3.
16. **Vohs JL**, **Chambers RA**, **O'Donnell BF**, **Krishnan GP**, **Morzorati SL.** Auditory steady state responses in a schizophrenia rat model probed by excitatory/inhibitory receptor manipulation. *Int J Psychophysiol* 86: 136–142, 2012. doi:10.1016/j.ijpsycho.2012.04.002.
17. **Sivarao DV**, **Chen P**, **Senapati A**, **Yang Y**, **Fernandes A**, **Benitex Y**, **Whiterock V**, **Li Y-W**, **Ahlijanian MK.** 40 Hz auditory steady-state response is a pharmacodynamic biomarker for cortical NMDA receptors. *Neuropsychopharmacology* 41: 2232–2240, 2016. doi:10.1038/npp.2016.17.
18. **Javitt DC**, **Sweet RA.** Auditory dysfunction in schizophrenia: integrating clinical and basic features. *Nat Rev Neurosci* 16: 535–550, 2015. doi:10.1038/nrn4002.
19. **Leishman E**, **O'Donnell BF**, **Millward JB**, **Vohs JL**, **Rass O**, **Krishnan GP**, **Bolbecker AR**, **Morzorati SL.** Phencyclidine disrupts the auditory steady state response in rats. *PLoS One* 10: e0134979, 2015. doi:10.1371/journal.pone.0134979.
20. **Schuelert N**, **Dorner-Ciossek C**, **Brendel M**, **Rosenbrock H.** A comprehensive analysis of auditory event-related potentials and network oscillations in an NMDA receptor antagonist mouse model using a novel wireless recording technology. *Physiol Rep* 6: e13782, 2018. doi:10.14814/phy2.13782.
21. **Raza MU**, **Sivarao DV.** Test-retest reliability of tone- and 40 Hz train-evoked gamma oscillations in female rats and their sensitivity to low-dose NMDA channel blockade. *Psychopharmacology (Berl)* 238: 2325–2334, 2021. doi:10.1007/s00213-021-05856-1.
22. **Sullivan EM**, **Timi P**, **Elliot Hong L**, **O'Donnell P.** Effects of NMDA and GABA-A receptor antagonism on auditory steady-state synchronization in awake behaving rats. *Int J Neuropsychopharmacol* 18: pyu118, 2015. doi:10.1093/ijnp/pyu118.
23. **Balla A**, **Ginsberg S**, **Abbas AI**, **Sershen H**, **Javitt DC.** Translational neurophysiological biomarkers of N-methyl-D-aspartate receptor dysfunction in serine racemase knockout mice. *Biomark Neuropsychiatry* 2: 100019, 2020. doi:10.1016/j.bionps.2020.100019.
24. **Kesby JP**, **Eyles DW**, **McGrath JJ**, **Scott JG.** Dopamine, psychosis and schizophrenia: the widening gap between basic and clinical neuroscience. *Transl Psychiatry* 8: 30, 2018. doi:10.1038/s41398-017-0071-9.
25. **Quednow BB**, **Geyer MA**, **Halberstadt AL.** Serotonin and schizophrenia. In: *Handbook of the Behavioral Neurobiology of Serotonin*, edited by Müller CR, Jacobs B**.** Academic Press, 2020, vol. 31, p. 711–743.
26. **Vejmola Č**, **Tylš F**, **Piorecká V**, **Koudelka V**, **Kadeřábek L**, **Novák T**, **Páleníček T.** Psilocin, LSD, mescaline, and DOB all induce broadband desynchronization of EEG and disconnection in rats with robust translational validity. *Transl Psychiatry* 11: 506–508, 2021. doi:10.1038/s41398-021-01603-4.
27. **Viktorin V**, **Griškova-Bulanova I**, **Voicikas A**, **Dojčánová D**, **Zach P**, **Bravermanová A**, **Andrashko V**, **Tylš F**, **Korčák J**, **Viktorinová M**, **Koudelka V**, **Hájková K**, **Kuchař M**, **Horáček J**, **Brunovský M**, **Páleníček T.** Psilocybin—Mediated Attenuation of gamma band auditory steady-state responses (ASSR) is driven by the intensity of cognitive and emotional domains of psychedelic experience. *J Pers Med* 12: 1004–1014, 2022. doi:10.3390/jpm12061004.
28. **Kozono N**, **Okamura A**, **Honda S**, **Matsumoto M**, **Mihara T.** Gamma power abnormalities in a Fmr1-targeted transgenic rat model of fragile X syndrome. *Sci Rep* 10: 18799–18799, 2020. doi:10.1038/s41598-020-75893-x.
29. **Ross B**, **Herdman AT**, **Pantev C.** Right hemispheric laterality of human 40 Hz auditory steady-state responses. *Cereb Cortex* 15: 2029–2039, 2005. doi:10.1093/cercor/bhi078.
30. **Kumar N**, **Jaiswal A**, **Roy D**, **Banerjee A.** Effective networks mediate right hemispheric dominance of human 40 Hz auditory steady-state response. *Neuropsychologia* 184: 108559, 2023. doi:10.1016/j.neuropsychologia.2023.108559.
31. **Bureš Z**, **Pysanenko K**, **Syka J.** Differences in auditory temporal processing in the left and right auditory cortices of the rat. *Hear Res* 430: 108708, 2023. doi:10.1016/j.heares.2023.108708.
32. **Fitch RH**, **Brown CP**, **O'Connor K**, **Tallal P.** Functional lateralization for auditory temporal processing in male and female rats. *Behav Neurosci* 107: 844–850, 1993. doi:10.1037//0735-7044.107.5.844.
33. **Paxinos G**, **Watson C.** *The Rat Brain in Stereotaxic Coordinates* (7th Eds.). Elsevier Inc, 2014.
34. **Tada M**, **Kirihara K**, **Ishishita Y**, **Takasago M**, **Kunii N**, **Uka T**, **Shimada S**, **Ibayashi K**, **Kawai K**, **Saito N**, **Koshiyama D**, **Fujioka M**, **Araki T**, **Kasai K.** Global and parallel cortical processing based on auditory gamma oscillatory responses in humans. *Cereb Cortex* 31: 4518–4532, 2021. doi:10.1093/cercor/bhab103.
35. **Li S**, **Hu R**, **Yan H**, **Chu L**, **Qiu Y**, **Gao Y**, **Li M**, **Li J.** 40-Hz auditory steady-state response deficits are correlated with the severity of persistent auditory verbal hallucination in patients with schizophrenia. *Psychiatry Res Neuroimaging* 336: 111748, 2023. doi:10.1016/j.pscychresns.2023.111748.
36. **Spencer KM**, **Niznikiewicz MA**, **Nestor PG**, **Shenton ME**, **McCarley RW.** Left auditory cortex gamma synchronization and auditory hallucination symptoms in schizophrenia. *BMC Neurosci* 10: 85, 2009. doi:10.1186/1471-2202-10-85.
37. **Erkizia-Santamaría I**, **Alles-Pascual R**, **Horrillo I**, **Meana JJ**, **Ortega JE.** Serotonin 5-HT2A, 5-HT2C and 5-HT1A receptor involvement in the acute effects of psilocybin in mice: in vitro pharmacological profile and modulation of thermoregulation and head-twitch response. *Biomed Pharmacother* 154: 113612, 2022. doi:10.1016/j.biopha.2022.113612.
38. **McFadden KL**, **Steinmetz SE**, **Carroll AM**, **Simon ST**, **Wallace A**, **Rojas DC.** Test–retest reliability of the 40 Hz EEG auditory steady-state response. *PLoS One* 9: e85748, 2014. doi:10.1371/journal.pone.0085748.
39. **Legget KT**, **Hild AK**, **Steinmetz SE**, **Simon ST**, **Rojas DC.** MEG and EEG demonstrate similar test–retest reliability of the 40 Hz auditory steady-state response. *Int J Psychophysiol* 114: 16–23, 2017. doi:10.1016/j.ijpsycho.2017.01.013.
40. **López-Giménez JF**, **Mengod G**, **Palacios JM**, **Vilaró MT.** Selective visualization of rat brain 5-HT2A receptors by autoradiography with [3H]MDL 100,907. *Naunyn Schmiedebergs Arch Pharmacol* 356: 446–454, 1997. doi:10.1007/pl00005075.
41. **Cornea-Hébert V**, **Riad M**, **Wu C**, **Singh SK**, **Descarries L.** Cellular and subcellular distribution of the serotonin 5-HT2A receptor in the central nervous system of adult rat. *J Comp Neurol* 409: 187–209, 1999. doi:10.1002/(sici)1096-9861(19990628)409:2<187::aid-cne2>3.0.co;2-p.

42. **Nissen TD**, **Laursen B**, **Viardot G**, **l'Hostis P**, **Danjou P**, **Sluth LB**, **Gram M**, **Bastlund JF**, **Christensen SR**, **Drewes AM.** Effects of vortioxetine and escitalopram on electroencephalographic recordings – A randomized, crossover trial in healthy males. *Neuroscience* 424: 172–181, 2020. doi:10.1016/j.neuroscience.2019.09.039.
43. **Tao X**, **Croom K**, **Newman-Tancredi A**, **Varney M**, **Razak KA.** Acute administration of NLX-101, a serotonin 1A receptor agonist, improves auditory temporal processing during development in a mouse model of fragile X syndrome. *J Neurodev Disord* 17: 1–18, 2025. doi:10.1186/s11689-024-09587-0.
44. **Sehatpour P**, **Javitt DC**, **De Baun HM**, **Carlson M**, **Beloborodova A**, **Margolin DH**, **Carlton MBL**, **Brice NL**, **Kantrowitz JT.** Mismatch negativity as an index of target engagement for excitation/inhibition-based treatment development: a double-blind, placebo-controlled, randomized, single-dose cross-over study of the serotonin type-3 receptor antagonist CVN058. *Neuropsychopharmacology* 47: 711–718, 2022. doi:10.1038/s41386-021-01170-8.
45. **Wetzel W**, **Ohl FW**, **Scheich H.** Global versus local processing of frequency-modulated tones in gerbils: An animal model of lateralized auditory cortex functions. *Proc Natl Acad Sci USA* 105: 6753–6758, 2008. doi:10.1073/pnas.0707844105.
46. **Levy RB**, **Marquarding T**, **Reid AP**, **Pun CM**, **Renier N**, **Oviedo HV.** Circuit asymmetries underlie functional lateralization in the mouse auditory cortex. *Nat Commun* 10: 2783, 2019. doi:10.1038/s41467-019-10690-3.
47. **Melynyte S**, **Pipinis E**, **Genyte V**, **Voicikas A**, **Rihs T**, **Griskova-Bulanova I.** 40 Hz auditory steady-state response: the impact of handedness and gender. *Brain Topogr* 31: 419–429, 2018. doi:10.1007/s10548-017-0611-x.
48. **Aghajanian GK**, **Marek GJ.** Serotonin model of schizophrenia: emerging role of glutamate mechanisms. *Brain Res Brain Res Rev* 31: 302–312, 2000. doi:10.1016/s0165-0173(99)00046-6.
49. **Vejmola Č**, **Šíchová K**, **Syrová K**, **Janečková L**, **Koudelka V**, **Tesař M**, **Nikolič M**, **Viktorinová M**, **Tylš F**, **Korčák J**, **Viktorin V**, **Kelemen E**, **Nekovářová T**, **Brunovský M**, **Horáček J**, **Kuchař M**, **Páleníček T.** Cross-species evidence for psilocin-induced visual distortions: apparent motion is perceived by both humans and rats. *Biol Psychiatry Glob Open Sci* 5: 100524, 2025. doi:10.1016/j.bpsgos.2025.100524.
50. **Coffman BA**, **Ren X**, **Longenecker J**, **Torrence N**, **Fishel V**, **Seebold D**, **Wang Y**, **Curtis M**, **Fowler L**, **Rhorer H**, **Kavanagh J**, **Lopez-Caballero F**, **Sklar A**, **Salisbury DF.** Lateralization of auditory steady state response (ASSR) deficits in first-episode schizophrenia - Effects of attention and associations with auditory hallucination severity. *J Psychiatr Res* 192: 424–432, 2026. doi:10.1016/j.jpsychires.2025.11.004.
51. **Roach BJ**, **Hirano Y**, **Ford JM**, **Spencer KM**, **Mathalon DH.** Phase delay of the 40 Hz auditory steady-state response localizes to left auditory cortex in schizophrenia. *Clin EEG Neurosci* 54: 370–378, 2023. doi:10.1177/15500594221130896.
52. **Parciauskaite V**, **Bjekic J**, **Griskova-Bulanova I.** Gamma-range auditory steady-state responses and cognitive performance: a systematic review. *Brain Sci* 11: 217, 2021. doi:10.3390/brainsci11020217.
53. **Manju V**, **Gopika KK**, **Arivudai Nambi PM.** Association of auditory steady state responses with perception of temporal modulations and speech in noise. *ISRN Otolaryngol* 2014: 374035–374038, 2014. doi:10.1155/2014/374035.
54. **Binder M**, **Górska U**, **Griskova-Bulanova I.** 40 Hz auditory steady-state responses in patients with disorders of consciousness: correlation between phase-locking index and coma recovery scale-revised score. *Clin Neurophysiol* 128: 799–806, 2017. doi:10.1016/j.clinph.2017.02.012.
55. **Binder M**, **Papiernik J**, **Griskova-Bulanova I**, **Frycz S**, **Chojnacki B**, **Górska-Klimowska U.** Diagnosing awareness in disorders of consciousness with gamma-band auditory responses. *Front Hum Neurosci* 17: 1243051, 2023. doi:10.3389/fnhum.2023.1243051.